Int. J. Electrochem. Sci., 7 **(2012)** 11091 - 11100

International Journal of ELECTROCHEMICAL SCIENCE
www.electrochemsci.org

Impedance Analysis of *Geobacter sulfurreducens* PCA, *Shewanella oneidensis* MR-1, and their Coculture in Bioeletrochemical Systems

Sokhee Jung[*]

Department of Civil and Environmental Engineering, The Pennsylvania State University, University Park, PA 16802, USA
[*]E-mail: sokheejung@gmail.com

Received: 9 May 2012 / *Accepted:* 29 September 2012 / *Published:* 1 November 2012

The impedance signatures of duplicate defined-culture bioanodes enriched with *Geobacter sulfurreducens*, *Shewanella oneidensis*, and their coculture were analyzed in microbial electrolyte cells. The PCA anodes and the MR-1 anodes had intracellular impedance (R_{IN}) a few orders of magnitude larger than extracellular impedance (R_{EX}), indicating intracellular exoelectrogenic process was a rate-limiting step. R_{IN} and R_{EX} of the PCA anodes were about 9-fold and 31 to 55-fold lower than those of the MR-1 anodes, respectively. Total capacitance was dominated by intracellular capacitance (C_{LF}) in both PCA and MR-1. Total capacitance of the MR-1 anodes was ~2.5 fold lower than for the PCA anodes. Different morphological features of high-frequency arcs were found in the defined cultures, suggesting impedance spectra can be utilized as electrochemical signature of different exoelectrogenic pathways.

Keywords: Geobacter sulfurreducens; Shewanella oneidensis MR-1; bioelectrochemistry; EIS

1. INTRODUCTION

Bioelectrochemical systems (BESs) utilize extracellular electron transfer reactions (exoelectrogenesis) to convert organic compounds into electricity [1-3], hydrogen [4, 5], and other valuable products [6, 7], simultaneous with performing biological wastewater treatment [8-10]. The bioanode is a crucial component in BESs for biological electricity generation [11]. It is composed of catalytic biofilm and conductive electrode [11]. Due to high complexity of the bioanode process, it is hard to elucidate its electrochemical reactions. However, researchers have sought more precise understanding of the bioanode process for improvement of bioanode performance [11].

In order to understand the bioanode process better, researchers have utilized electrochemical approach. Charge transfer resistance and capacitance of BESs were characterized by applying electrochemical impedance spectroscopy (EIS) [12-14] and by analyzing transient potential responses [15]. EIS is increasingly used to analyze the bioanode process due to its methodological convenience [13, 16-19]. It has been applied on mixed-culture anodes [20-23] and enzyme-immobilized anodes [14, 24]. Recently, demands for investigation of pure exoelectrogens (electricity producing bacteria) are increasing to characterize homogeneous exoelectrogenic reaction from a unique bacterial strain.

The two famous exoelectrogens, *G. sulfurreducens* PCA and *S. oneidensis* MR-1, have been studied intensively to elucidate the bioanode process. Both strains have very different electrochemical physiologies. Conductive protein pilus, *nanowire*, is the major appendage for electron transfer onto the anode surface in *G. sulfurreducens* whereas flavin, electron shuttle, is one for *S. oneidensis* (Fig. 2) [25-27]. For this reason, *G. sulfurreducens* lives on the anode electrode, but *S. oneidensis* favors suspended growth. Because major portion of electricity generation in BESs is associated with these two exoelectrogenic mechanisms, their precise understanding will definitely lead to the improvement of the bioanode performance.

For better understanding their electrophysiology, simple voltammetry was performed on them [25, 28]. However, their impedance in BESs has never been comparatively explored before. So, we analyzed impedance of bioanodes inoculated with *G. sulfurreducens*, *S. oneidensis*, and their coculture in duplicate in this study. Charge transfer resistance and capacitance in each step of the exoelectrogenesis were successfully measured using *G. sulfurreducens* and *S. oneidensis* in BES. And their coculture impedance signature was also explored. Results reported here expand our understanding of the bioanode process, which can be used for improvement of BES performance [11, 23].

2. MATERIALS AND METHODS

2.1. Bacterial growth and BES construction

Duplicate two-chamber fuel cells were constructed as previously with some modifications (Fig. 1) [22] The ends of each tube were glued with silicon (Loctite Superflex Cat. 59530), attached with anion exchange membrane (AMI-7001, Membrane International Inc.), and assembled with a pinch clamp. Anode mouth and sampling port were sealed with butyl-rubber stoppers, and clamped with an aluminum cap. Anode electrodes (2.5 cm× 6 cm, 30 cm^2) were made of carbon cloth (BASF Fuel Cell Inc.) and cathode electrodes (2.5×6 cm) were made by applying platinum (0.5 mg/cm^2 Pt) and four diffusion layers on a 30 wt % wet-proofed carbon cloth (type B-1B, E-TEK) as previously described [29].

G. sulfurreducens strain PCA (ATCC 51573) was purchased from ATCC and *S. oneidensis* strain MR-1 was donated from Dr. Daniel Bond (Associate Professor, University of Minnesota). For inoculation, suspended bacteria were grown in defined media as previously described [30, 31]. Acetic acid (10 mM) was added as the electron donor for PCA, and lactic acid (10 mM) was added for MR-1 and for the coculture. For anode medium, the 50 mM of fumarate was replaced with NaCl (2.9 g/L, 50

mM) to maintain osmolality and conductivity [31]. Final medium pH was 6.8. Cathode medium contained 0.6 g Na_2HPO_4, 1.5 g of NH_4Cl, 0.1 g of KCl, 2.9 g/L of NaCl, and 2.5 g of $NaHCO_3$.

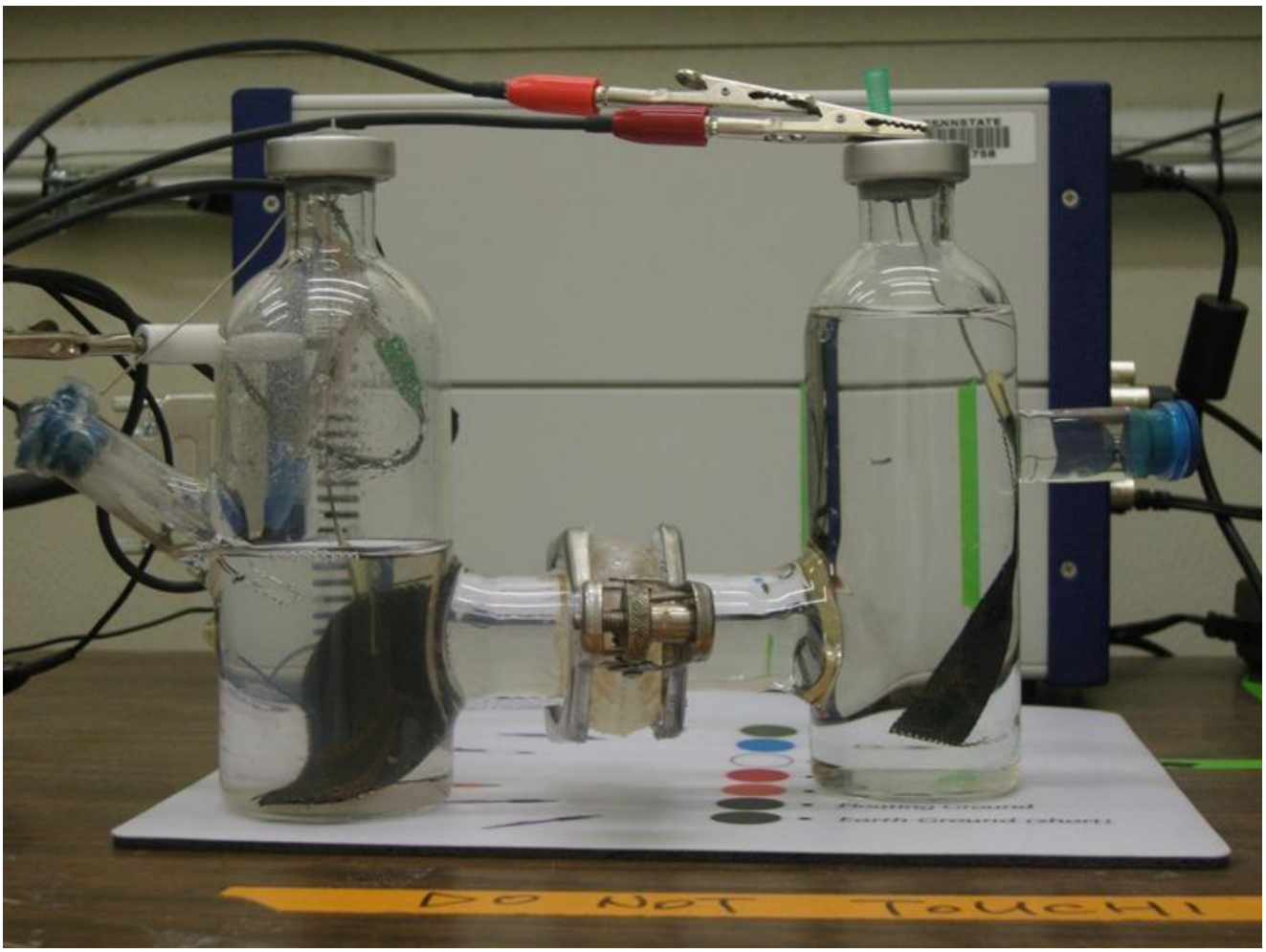

Figure 1. Two-chamber microbial electrolyte cell (MEC) used for this experiment. A left chamber is an anode chamber and a right chamber is a cathode chamber.

Suspended cells (50 ml) were centrifuged (× 9000 cfg) for 15 min at 5 °C, resuspended in 10 ml of the medium. For the coculture reactors, 50-ml cells for each strain was centrifuged and resuspended in each 5-ml medium. They were inoculated into the anode chamber, containing 120-mL medium. The cathode chamber was filled with 220-ml medium. Circuits were connected through 460 Ω of external resistor. The cathode chamber was provided with air passed through a 0.45-μm-pore-size filter. The reactors were operated for ~ 150 hours in the first batch, and electrochemical measurement was performed in the second batch as described below. All experiments were performed at 30 °C.

2.2. Electrochemical measurement

Cyclic voltammetry (CV) and EIS were performed using a potentiostat Reference 600 (Gamry Instrument Inc.). Before measurements, the reactors were operated for 2 hours to stabilize the bioanode

in the fresh medium condition at -0.2 V (vs. Ag/AgCl). The circuit was disconnected for 30 min to create open circuit potential, and anodic CV was performed with the following conditions: scan rate 1 mV/sec, step size 1 mV, Auto I/E Range, Scan limits -0.6 and 0.1 V.

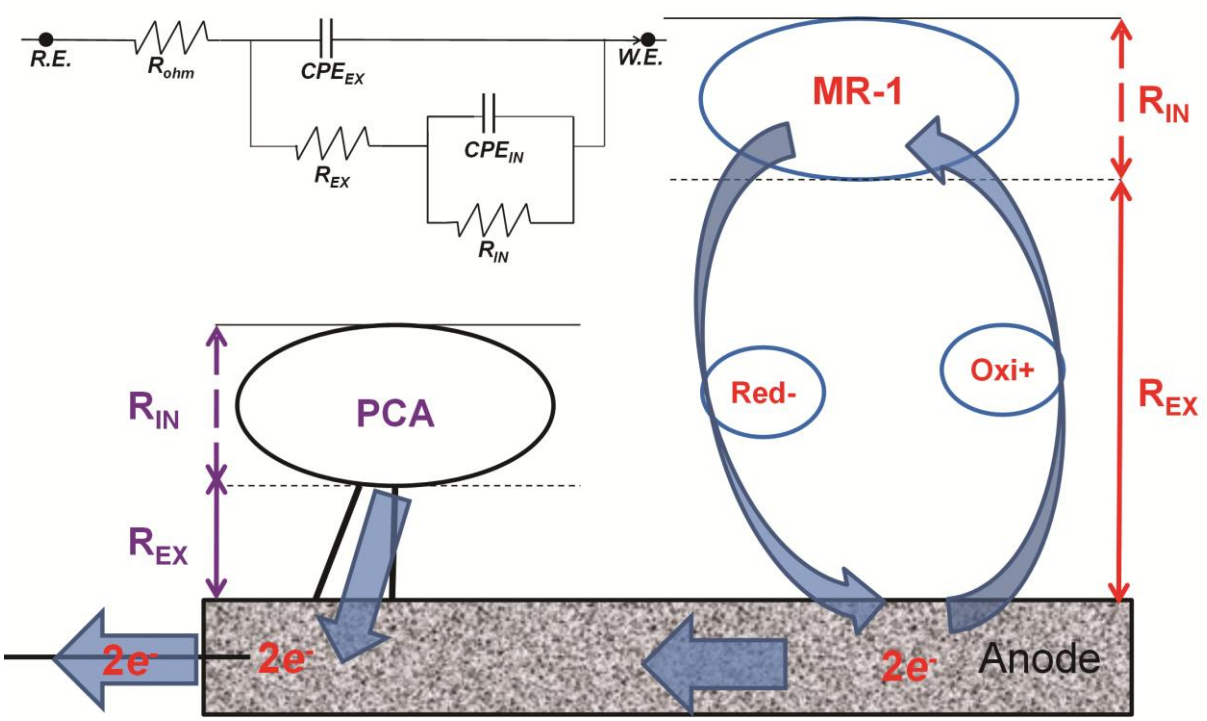

Figure 2. Schematics of exoelectrogenic mechanisms of G. sulfurreducens PCA (PCA) and S. oneidensis MR-1 (MR-1) on the anode surface and the equivalent circuit model (upper-left) used to model their impedance parameters. EX: extracellular process, IN: intracellular process, [Red-]: reduced electron shuttle, [Oxi+]: oxidized electron shuttle, R: impedance, CPE: constant phase element, R.E.: reference electrode, W.E.: working electrode.

For potentiostatic EIS, the anode electrodes were poised at -0.4 V for 30 minutes. And EIS was performed with following conditions: AC voltage 10 mV rms, initial frequency 103 kHz, final frequency 50 mHz, 10 points/decade, and -0.4 V of DC voltage.

Impedance spectra were fitted into the equivalent circuit model in previous studies [13, 32] by $\chi 2$-minimization using Echem Analyst (Gamry Instrument Inc.). The equivalent circuit model consists of two successive RC time constants (Fig. 2) [13]. A constant phase element (CPE) was incorporated to model a non-ideal capacitor, defined as $1/Z = T(j\ \omega)^{\alpha}$, where $T\ (S \cdot s^{\alpha})$ is a numerical value of the admittance $(1/|Z|)$ at $\omega = 1$, α is an empirical nonideality constant, and $\omega\ (s^{-1})$ is the radial frequency $(\omega = 2\pi f)$ [33]. Capacitance (C) was calculated using $C = (TR_p)^{1/\alpha}/R_p$, where R_p (Ω) is the charge transfer resistance (or polarization resistance). Potential values were reported with respect to the Ag/AgCl reference electrode.

3. RESULTS AND DISCUSSION

3.1. Start-up and CV

In the start-up, all reactors produced current immediately as circuits were connected.

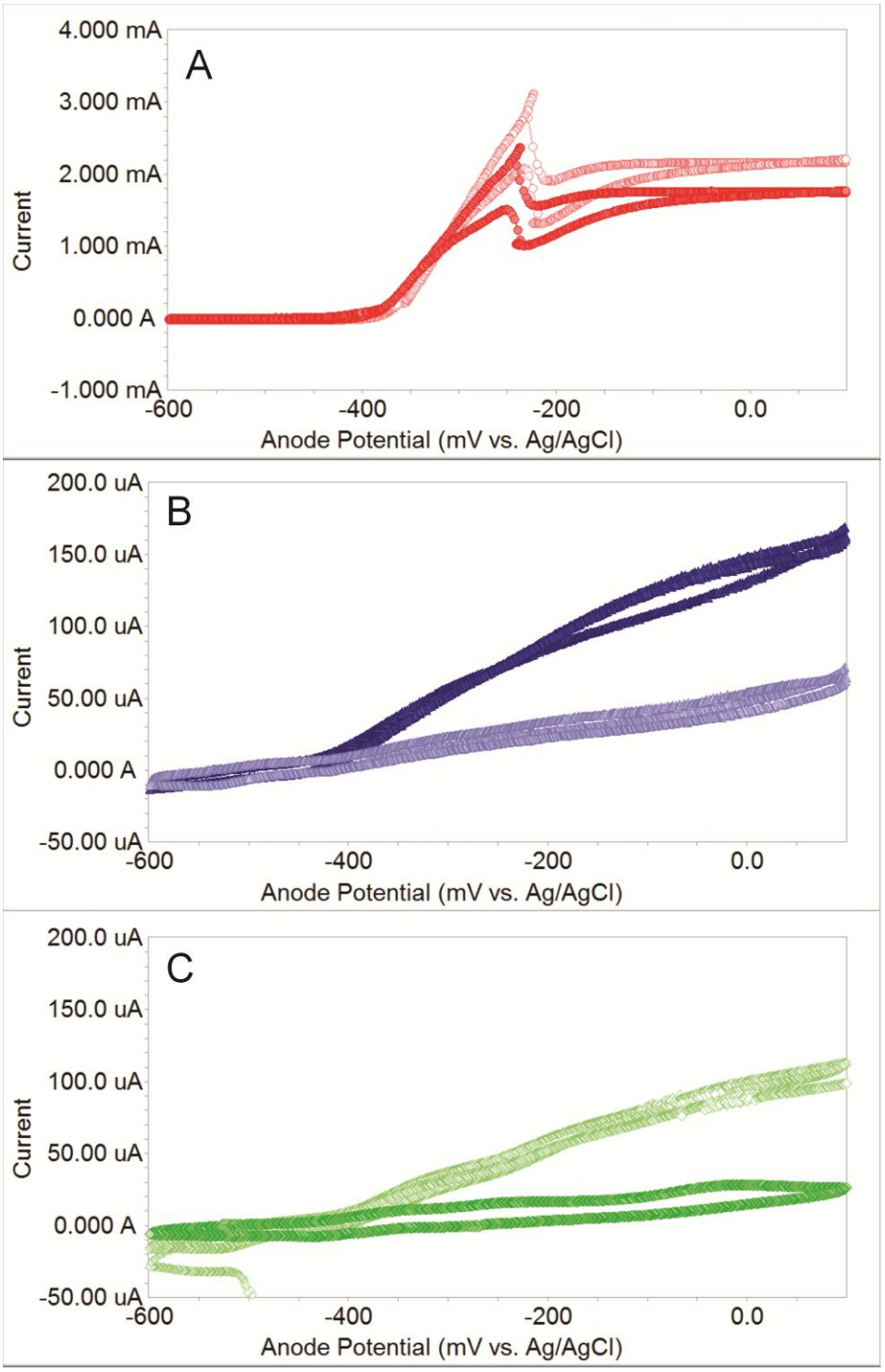

Figure 3. CV curves of anodes inoculated with PCA (A), MR-1 (B), or their coculture (C).

Current developed rapidly in the PCA reactors, followed by the coculture reactors and the MR-1 reactors. Anodic CVs showed the PCA anodes generated 2.72 ± 0.54 mA and the MR-1 anodes generated 0.12 ± 0.07 mA (Fig. 3). Binary extracellular electron transfers in the coculture reactors were expected to increase current production. However, the coculture anodes was fed with lactate only and produced lower current (68 ± 61 μA) possibly because slow lactate oxidation of MR-1 could not provide enough acetate for PCA. Acetate is an anaerobic end product of the lactate oxidation of MR-1. Impedance measured at open circuit potential was reported to produce misleading results because living bacterial biofilm on the anode surface cannot respire at open circuit [13, 19]. For fair comparative evaluation, EIS was performed at -400 mV of anode potential where similar levels of current (≈ 10 μA) were produced in the three BES conditions.

3.2. EIS analysis

In both the PCA anodes and the MR-1 anodes, the intracellular process had higher values of impedance (R), capacitance (C), and non-ideality constant (α) than the extracellular process (Table 1 and Fig. 4). Intracellular impedances (R_{IN}) occupied ~80% of total impedance in the exoelectrogenic electron transfer in the PCA and ~95% in the MR-1. In other words, R_{IN} were ~230 - 450% larger than R_{EX} in the PCA and ~1750 - 1950% larger in the MR-1, indicating the intracellular process was a rate-limiting step in the both bacterial strains. Total capacitance was predominated by intracellular capacitance (C_{IN}) in the both conditions. It shows almost all electrical charges involved in the exoelectrogenic electron transfer reside in the intracellular reaction step, indicating that far more electrochemical reactions possibly occurs in the intracellular process than in the extracellular process. Improved the bioanode current generation would be feasible through enhanced anodic bacterial metabolism by physiological optimization or genetic engineering.

EIS revealed that nanowire-utilizing PCA and flavin-utilizing MR-1 for their exoelectrogenic electron transfer had very different impedance characteristics (Table 1 and Fig. 4). R_{IN} and R_{EX} in the PCA were only ~11% and only ~2-3% of those in the MR-1, respectively. To sum up, total charge transfer impedance in the PCA were only ~10% of that in the MR-1, indicating PCA alleviated electron transfer resistance using nanowires much better than MR-1. For exoelectrogenesis of MR-1, flavins should diffuse through cellular membranes and undergo their oxidation and reduction. This complex remote redox process of MR-1 creates ~40 time larger electrical resistance and subsequent energetic loss in MR-1 as indicated by the R_{EX} values. However, the electron transfer via the conductive protein wires of PCA drastically reduces electrical resistance and energetic loss during the exoelectrogenesis in the bioanode as indicated by these impedance measurements.

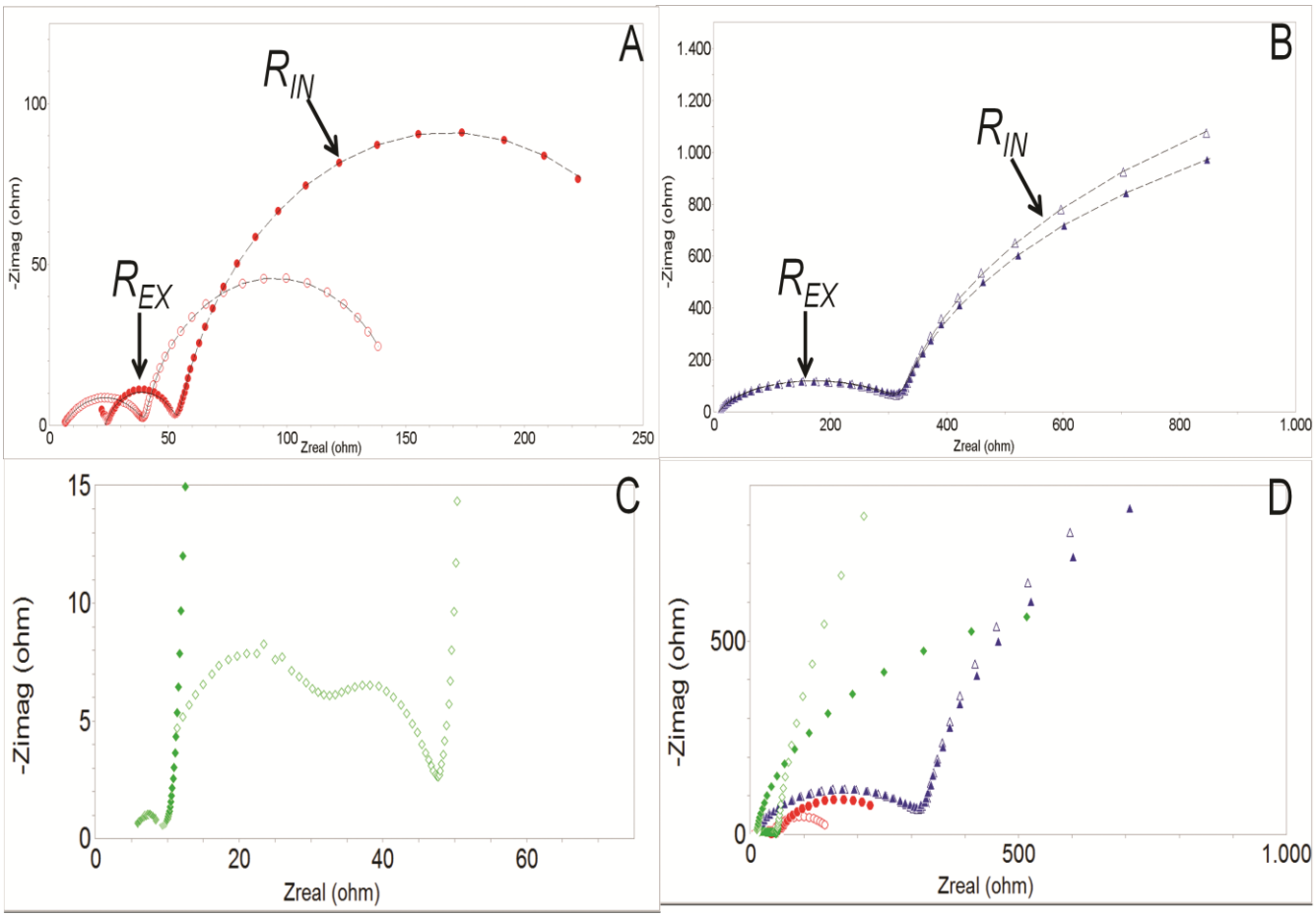

Figure 4. Nyquist plots of anodes inoculated with PCA (A), MR-1 (B), or their coculture (C). Their composite plots are shown in (D).

MR-1 can produce nanowires [34], but current generations of MR-1 is highly dependent on the flavin mediation [25]. C_{IN} in the PCA were ~170 - 190% larger than that in the MR-1, indicating more electrical charges involves in the intracellular process in the electron transfer of PCA. However, C_{EX} in the PCA were ~5-22% of that in the MR-1, showing less electrical charges involves in the extracellular process of PCA.

Conclusively, these results show that PCA harbors exoelectrogenic machinery more energy-efficient and more conductive. Previous investigation also demonstrated that PCA had 10 time higher current density (3 A/m^2) than MR-1 (0.3 A/m^2) at ~0 mV of anode potential in BESs [25, 28]. However, only C_{EX} values seem not concur with the other supporting evidences. Because PCA is able to transfer 10 time higher current density, one might think that C_{EX} of PCA should be higher than MR-1. During the electron transfer mediated by flavins in MR-1, flavins diffuse out into medium or other non-relevant surfaces to the electricity generation in BES [25, 27]. This substantially decreases electron recovery. So, even though MR-1 has higher C_{EX}, it produces lower current due to its low electron recovery originated from flavin diffusions.

Table 1. Calculated impedance parameters of bioanodes at -400 mV of anode potential (n=2). Impedance (R), capacitance (C), and nonideality constant (α)

	PCA (1)	PCA (2)	MR-1 (1)	MR-1 (2)
R_{EX} (Ω)	36.1 ± 1.7	35.0 ± 5.8	319.6 ± 4.7	323.9 ± 4.9
R_{IN} (Ω)	120.0 ± 15.2	192.4 ± 50.1	6555 ± 4045	5997 ± 4443
$\sum R$ (Ω)[1)]	156.0 ± 16.9	227.3 ± 44.4	6875 ± 4040	6321 ± 4439
C_{EX} (μF)	1.3 ± 0.0	5.0 ± 0.4	23 ± 3	27 ± 4
C_{IN} (mF)	9.08 ± 1.51	9.30 ± 1.76	3.42 ± 0.02	3.25 ± 0.01
$\sum C$ (mF)[2)]	9.08 ± 1.51	9.31 ± 1.76	3.44 ± 0.01	3.28 ± 0.01
α_{EX}	0.57 ± 0.01	0.75 ± 0.01	0.73 ± 0.01	0.80 ± 0.00
α_{IN}	0.91 ± 0.03	0.85 ± 0.01	0.96 ± 0.01	0.94 ± 0.01
Goodness of fit	2.6×10^{-5} ± 0.6×10^{-5}	2.0×10^{-5} ± 0.4×10^{-5}	4.3×10^{-4} ± 0.4×10^{-4}	4.3×10^{-4} ± 0.3×10^{-4}

1) For serially-connected resistors, $\sum R = R_{EX} + R_{IN}$
2) For parrarelly-connected capacitors, $\sum C = C_{EX} + C_{IN}$

Different morphologies of high-frequency arcs were created from the three culture conditions. In particular, Nyquist plots of the coculture anode had a unique high-frequency arc consisting of two semi arcs (Fig. 4-C). The MR-1 anodes had larger high-frequency arcs than those of the PCA anodes. While those have a semicircle shape with a different radius, high-frequency arcs of the coculture anodes consisted of two small sub-arcs. This finding implies impedance spectra might be applied to distinguish exoelectrogenic electron transfer mechanisms.

4. CONCLUSION

CV (scan limits -0.6 and 0.1 V) tests showed PCA, MR-1, and their coculture produced 2.72 ± 0.54 mA, 0.12 ± 0.07 mA, and 68 ± 61 μA, respectively. The PCA anodes and the MR-1 anodes had R_{IN} a few orders of magnitude larger than R_{EX}. R_{IN} and R_{EX} of the PCA anodes were about 9-fold and

31 to 55-fold lower than those of the MR-1 anodes, respectively. Total capacitance was dominated by C_{IN} in both PCA and MR-1. Total capacitance of the PCA anodes was ~2.5 fold higher than for the MR-1 anodes. Different morphologies of high-frequency arcs were created from the three culture conditions, suggesting EIS might be used as an electrochemical fingerprinting method to identify exoelectrogenic pathway.

ACKNOWLEDGEMENTS

The authors thank Dr. John M. Regan (Professor, Department of Civil and Environmental Engineering, Penn State University) for his support. We also thank Mr. Sangkwon Lee (Material Science and Engineering, Penn State University) for his help. This research was supported by Fellowship from National Research Foundation of Korea and Scholarship from Korean-American Scientists and Engineers Association.

References

1. B.E. Logan, J.M. Regan, *Environ Sci Technol*, 40 (2006) 5172-5180.
2. J.R. Kim, G.C. Premier, F.R. Hawkes, R.M. Dinsdale, A.J. Guwy, *J Power Sources*, 187 (2009) 393-399.
3. B. Min, I. Angelidaki, *J Power Sources*, 180 (2008) 641-647.
4. K.-J. Chae, M.-J. Choi, J. Lee, F.F. Ajayi, I.S. Kim, *Int J Hydrogen Energ*
33 (2008) 5184-5192.
5. R.A. Rozendal, H.V.M. Hamelers, G.J.W. Euverink, S.J. Metz, C.J.N. Buisman, *Int J Hydrogen Energ*
31 (2006) 1632-1640.
6. R.A. Rozendal, E. Leone, J.g. Keller, K. Rabaey, *Electrochem Commun*, 11 (2009) 1752-1755.
7. H.J. Jeon, K.-w. Seo, S.H. Lee, Y.-H. Yang, R.S. Kumaran, S. Kim, S.W. Hong, Y.S. Choi, H.J. Kim, *Bioresource Technol*, 109 (2012) 308-311.
8. P. Aelterman, K. Rabaey, P. Clauwaert, W. Verstraete, *Water Sci Technol*, 54 (2006) 9-15.
9. R.A. Rozendal, H.V.M. Hamelers, K. Rabaey, J. Keller, C.J.N. Buisman, *Trends Biotechnol*, 26 (2008) 450-459.
10. A. Gurung, J. Kim, S. Jung, B.-H. Jeon, J. Yang, S.-E. Oh, *Biotechnol Lett*, (2012) 1-7.
11. S. Jung, J.M. Regan, *Appl. Environ. Microbiol.*, 77 (2011) 564-571.
12. H.D. Yoo, J.H. Jang, B.H. Ka, C.K. Rhee, S.M. Oh, *Langmuir*, 25 (2009) 11947-11954.
13. S. Jung, M.M. Mench, J.M. Regan, *Environ Sci Technol*, 45 (2011) 9069-9074.
14. S. Ouitrakul, M. Sriyudthsak, S. Charojrochkul, T. Kakizono, *Biosens Bioelectron*, 23 (2007) 721-727.
15. P.T. Ha, H. Moon, B.H. Kim, H.Y. Ng, I.S. Chang, *Biosens Bioelectron*, 25 (2010) 1629-1634.
16. A.P. Borole, D. Aaron, C.Y. Hamilton, C. Tsouris, *Environ Sci Technol*, 44 (2010) 2740-2745.
17. A.K. Manohar, O. Bretschger, K.H. Nealson, F. Mansfeld, *Bioelectrochemistry*, 72 (2008) 149-154.
18. R.P. Ramasamy, Z.Y. Ren, M.M. Mench, J.M. Regan, *Biotechnol Bioeng*, 101 (2008) 101-108.
19. G.S. Frankel, M. Rohwerder, Electrochemical Techniques for Corrosion, in: Encyclopedia of Electrochemistry, Wiley-VCH Verlag GmbH & Co. KGaA, 2007.
20. D.R. Bond, D.E. Holmes, L.M. Tender, D.R. Lovley, *Science*, 295 (2002) 483-485.
21. D.E. Holmes, D.R. Bond, R.A. O'Neil, C.E. Reimers, L.R. Tender, D.R. Lovley, *Microb Ecol*, 48 (2004) 178-190.
22. S. Jung, J.M. Regan, *Appl Microbiol Biotechnol*, 77 (2007) 393-402.
23. B.E. Logan, J.M. Regan, *Trends Microbiol*, 14 (2006) 512-518.

24. J. Shim, G.-Y. Kim, S.-H. Moon, *J Electroanal Chem*, 653 (2011) 14-20.
25. E. Marsili, D.B. Baron, I.D. Shikhare, D. Coursolle, J.A. Gralnick, D.R. Bond, *Proc Natl Acad Sci U S A*, 105 (2008) 3968-3973.
26. G. Reguera, K.D. McCarthy, T. Mehta, J.S. Nicoll, M.T. Tuominen, D.R. Lovley, *Nature*, 435 (2005) 1098-1101.
27. H. von Canstein, J. Ogawa, S. Shimizu, J.R. Lloyd, *Appl. Environ. Microbiol.*, 74 (2008) 615-623.
28. E. Marsili, J.B. Rollefson, D.B. Baron, R.M. Hozalski, D.R. Bond, *Appl. Environ. Microbiol.*, 74 (2008) 7329-7337.
29. S. Cheng, H. Liu, B.E. Logan, *Electrochem Commun*, 8 (2006) 489-494.
30. M. Lanthier, K.B. Gregory, D.R. Lovley, *FEMS Microbiol Lett*, 278 (2008) 29-35.
31. D.R. Lovley, E.J. Phillips, *Appl Environ Microbiol*, 54 (1988) 1472-1480.
32. S. Jung, Y.-H. Ahn, S.-E. Oh, J. Lee, K.T. Cho, Y. Kim, M.W. Kim, J. Shim, M. Kang, *Bull. Korean Chem. Soc.*, 33 (2012) 3349-3354.
33. J.R. Macdonald, *Ann Biomed Eng*, 20 (1992) 289-305.
34. Y.A. Gorby, S. Yanina, J.S. McLean, K.M. Rosso, D. Moyles, A. Dohnalkova, T.J. Beveridge, I.S. Chang, B.H. Kim, K.S. Kim, D.E. Culley, S.B. Reed, M.F. Romine, D.A. Saffarini, E.A. Hill, L. Shi, D.A. Elias, D.W. Kennedy, G. Pinchuk, K. Watanabe, S. Ishii, B. Logan, K.H. Nealson, J.K. Fredrickson, *Proc Natl Acad Sci U S A*, 103 (2006) 11358-11363.